Preparation of Porous PVDF Membrane via Thermally Induced Phase Separation with Diluent Mixture of DBP and DEHP

Gen-Liang Ji, Chun-Hui Du, Bao-Ku Zhu, You-Yi Xu

Department of Polymer Science and Engineering, Zhejiang University, Hangzhou 310027, China

Received 9 October 2006; accepted 18 February 2007
DOI 10.1002/app.26385
Published online 23 April 2007 in Wiley InterScience (www.interscience.wiley.com).

ABSTRACT: Poly(vinylidene fluoride) microporous membranes were prepared via the thermally induced phase separation process using diluent mixture of dibutyl phthalate (DBP) and di(2-ehylhexyl) phthalate (DEHP). The effects of the DBP ratio to DEHP in the diluent mixture on the phase diagrams were investigated. The phase diagrams can be controlled successfully by varying the DBP ratio in the diluent mixture. The compatibility between polymer and diluent mixture was characterized to explain the features in the phase diagram. The cross-sectional structures of membranes were investigated and related to the DBP ratio in diluent mixtures, initial polymer concentration, and cooling rate. When the DBP ratio to DEHP was 30 wt/70 wt, only spherulites structure was obtained at the polymer concentration of 30 wt % and at the cooling rate of 10°C/min, whereas the cellular structure was detected as the polymer concentration increased or the cooling rate deceased. In the case of the systems with only S-L phase separation, only spherulites structures were observed and the sizes of spherulites increased with increase in the polymer concentration and with decrease in the cooling rate. © 2007 Wiley Periodicals, Inc. J Appl Polym Sci 105: 1496–1502, 2007

Key words: PVDF; membrane; TIPS; compatibility; cross-sectional structure

INTRODUCTION

Poly(vinylidene fluoride) (PVDF) exhibits excellent chemical resistance, thermal stability, and intrinsic hydrophobicity that promote its use for membrane material. PVDF membranes have been widely used in organic/water separation,[1,2] membrane distillation,[3,4] ultrafiltration,[5] and fabrication of gel polymer electrolyte.[6,7] Preparation and characterization of PVDF membranes by dry/wet phase inversion processes were studied by many investigators,[8–13] but few studies have been reported on preparation of PVDF microporous membrane via thermally induced phase separation (TIPS) method.[14–16]

TIPS process is a well known method for obtaining membrane with controlled morphology,[17,18] and has several well-documented advantages, including (1) greater flexibility and ease of control than conventional casting process, (2) a very low tendency for defect formation, and (3) morphology characterized by very high overall porosity and effective control of the final pore size. In the TIPS process, homogeneous solution needs to be formed by the dissolution of a polymer in a diluent at high temperature, and phase separation is induced by the cooling of the polymer solution. When thermal energy is removed from a homogeneous polymer–diluent mixture, the TIPS can occur via Solid–Liquid (S-L) or Liquid–Liquid (L-L) phase separation depending on the polymer–diluent interaction, the polymer composition, and the thermal diving force. The final morphology of membrane in TIPS process depends upon the kinetics as well as the thermodynamics of the phase separations. The effects of the diluent on the structure of TIPS membranes were investigated for solid–liquid phase separation systems in terms of the diluent mobility and crystallization temperature.[19] Also the effects of the interaction parameter on the phase diagram and the final phase separated structure were studied by Vadalia et al.[20] In their work, diluent mixtures were used in preparing microporous membrane by TIPS of a ternary solution of HDPE, ditrydecylphthalate, and hexadecane. Considering the diluent mixture to be one component, the interaction between polymer and diluent was changed by the ratio of diluent mixture. Shang et al. used 1,3-propanediol and glycerol and their mixture as diluents in the preparation of poly(ethylene-*co*-vinyl alcohol) hollow-fiber membranes via TIPS method.[21] When 1,3-propanediol ratio increased in diluent mixture, the cloudy point shifted to lower

Correspondence to: C.-H. Du (duchunhui@zju.edu.cn) or (geegl1980@hotmail.com).

Contract grant sponsor: National Basic Research Program of China; contract grant number: 2003CB615705.

Contract grant sponsor: National Nature Science Foundation; contract grant number: 50433010.

temperatures; meanwhile, the membrane cross-structure changed from a cellular structure due to liquid–liquid phase separation to a particulate structure due to only polymer crystallization.

In this study, PVDF membranes were prepared along with diluent mixtures (dibutyl phthalate (DBP)/di(2-ehylhexyl) phthalate (DEHP)) via the TIPS method. The phase diagrams for PVDF/DBP/DEHP ternary blends were determined. The equilibrium phase diagram is considered a good tool for controlling the morphology and interpreting the membrane structure. The objective of this study was to demonstrate the effects of the DBP ratio in diluent mixture, polymer concentration, and cooling rate on the cross-sectional structures of membranes with the assistance of phase diagrams.

EXPERIMENTAL

Materials

The PVDF (M_n = 59,000, M_w/M_n = 2.88) used in the study was provided by Solvay Solexis (1012) with an MFI of 1.5. DBP and DEHP, supplied by Guangdong Guanghua Chemical Regent Co. and Shanghai Chemical Reagent Co., respectively, were used for preparing diluent mixtures without further purification. Since both DBP (bp 340°C) and DEHP (bp 386°C) have boiling points much higher than the melting point of PVDF (174°C), they were chosen to form diluent mixtures in preparing PVDF membrane via TIPS method.

Preparation of PVDF/DBP/DEHP blends

A mixture of known concentration of the two diluents (DBP, DEHP) was prepared beforehand. Since PVDF hardly dissolves in pure DEHP at higher temperature (240°C), the diluent mixtures with the ratio of DBP/DEHP over 27.5 wt/72.5 wt, in which PVDF dissolves more quickly to form homogenous solution at 240°C, were chosen as the latent diluents for this study. PVDF and the diluent mixtures were mixed at an elevated temperature (240°C) under nitrogen atmosphere for at least 3 h in a glass vessel with a stirrer. Then the glass vessel was quenched in liquid nitrogen to solidify the sample, and broken open to obtain the solid polymer–diluent sample.

Determination of the phase diagram

The cloudy point (T_{cloud}), crystallization temperature (T_c), and melting temperature (T_m) were measured according to the method reported by Shang et al.[21] The solid sample was chopped into small pieces and then placed between a pair of microscope cover slips. A Teflon film with a circle opening in the center was inserted between the cover slips to prevent diluent loss by evaporation. First the sample was

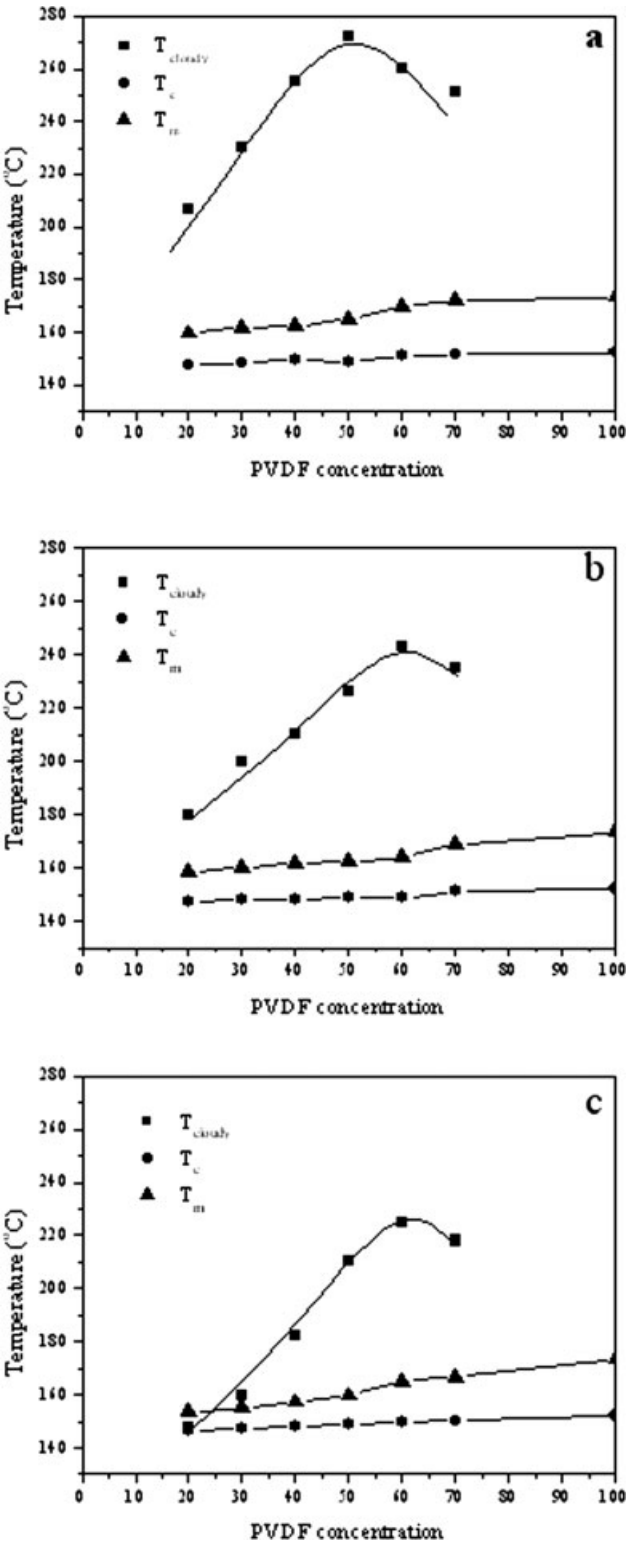

Figure 1 Phase diagrams with curves of L-L phase separation, crystallization, and melting for three systems of PVDF and diluent mixtures: (a) 27.5 wt/62.5 wt DBP/DEHP, (b) 30 wt/70 wt DBP/DEHP, (c) 32.5 wt/67.5 wt DBP/DEHP, obtained by optical microscopy and DSC at 10°C/min.

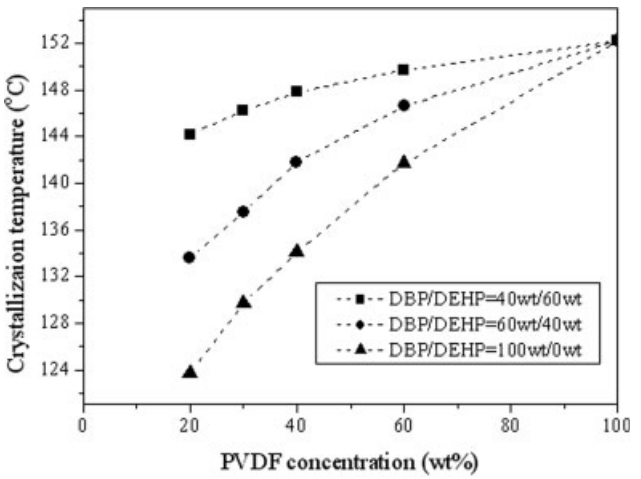

Figure 2 Crystallization curves for systems with only S-L phase separation, obtained by DSC at 10°C/min.

heated on a hot stage (Linkam THMS600) to 240°C at 10°C/min and held for 1 min, then cooled to 40°C at a rate of 10°C/min. T_{cloud} was determined visually by the appearance of turbidity under an optical microscope (Nikon eclipse E600 POL). The crystallization curve and melting curve were determined by a perkin–Elmer DSC-7. All DSC measurements were performed under the nitrogen atmosphere, and sample weights varied from 4 to 7 mg. The solid sample was sealed in an aluminum differential scanning calorimetry pan, melted at 240°C for 5 min to erase thermal history and cooled to 40°C at 10°C/min, and then heated to 240°C at 10°C/min again. The onset temperatures of the exothermic peak during the cooling and the endothermic peak during the heating were taken as the T_c and T_m, respectively.

Preparation of flat membrane

A homogeneous polymer–diluent sample was placed between a pair of microscope cover slips. The thickness of the membrane was adjusted by the insertion of the Teflon film (80 μm) between the slips. The sample was heated at 240°C for 1 min on the hot stage and cooled to 40°C at various cooling rate (5, 10, and 30°C/min). The diluent in the flat membrane was extracted by immersion in ethanol for 24 h. The final membrane was dried in the air.

Observation of the membrane cross section

For the cross section observation, the microporous membrane was freeze-fractured in liquid nitrogen and then sputter-coated (Hitachi® E1020) with gold. A field-emitting SEM (Sirion-100, FEI Co., Netherlands) was employed to examine the membrane cross section.

TABLE I
Density and Hansen Solubility Parameters for PVDF and Diluents

Substance	Density (g/cm^3)	δ_d ($MPa^{1/2}$)	δ_p ($MPa^{1/2}$)	δ_h ($MPa^{1/2}$)
DBP	1.045	17.8	8.6	4.1
DEHP	0.985	16.6	7	3.1
PVDF	1.78	17.2	12.5	9.2

RESULTS AND DISCUSSION

Phase diagram

As described in experimental, mixtures of DBP and DEHP with different DBP ratio were prepared to change the interaction between PVDF and the diluent mixture systematically. The experimental phase diagrams by optical microscopy and DSC for PVDF with three mixtures of DBP and DEHP (27.5/72.5, 30/70, and 32.5/67.5 wt/wt DBP/DEHP) are shown in Figure 1. The phase diagram for the system with 27.5 wt/72.5 wt DBP/DEHP is shown in Figure 1(a). Since PVDF is a semicrystalline polymer, the liquid–liquid phase separation existed simultaneously with a crystallization line in the phase diagram. The cloudy point (T_{cloud}) of PVDF/diluent mixture blend first shifted to higher temperature with polymer concentration increasing, went through a maximum centered at about 50 wt % polymer concentration, and then decreased. On the other hand, the crystallization temperature (T_c) was almost invariable and the melting temperature (T_m) increased slightly as the composition of PVDF in blend increased. These phenomena were also seen in diagrams for the system with 30 wt/70 wt and 32.5 wt/67.5 wt DBP/DEHP, as shown in Figures 1(b,c). The phase diagrams for these three systems, all of which had a region of L-L phase separation, exhibited the relationship between the cloudy point and the DBP ratio in diluent mixture. As shown in Figure 1, it was found that the cloud point curve shifted to lower temperatures with an insignificant effect on T_m and T_c as the DBP ratio increased. So it can be concluded that the L-L phase separation temperature is more sensitive to the DBP ratio in diluent mixture than the crystallization temperature in the system with L-L phase separation.

TABLE II
The Values of Solubility Parameter for Four Diluent Mixtures

Diluent mixture (wt/wt DBP/DEHP)	δ_d ($MPa^{1/2}$)	δ_p ($MPa^{1/2}$)	δ_h ($MPa^{1/2}$)
30/70	16.95	7.46	3.39
32.5/67.5	16.97	7.50	3.41
50/50	17.18	7.78	3.59
100/0	17.80	8.60	4.10

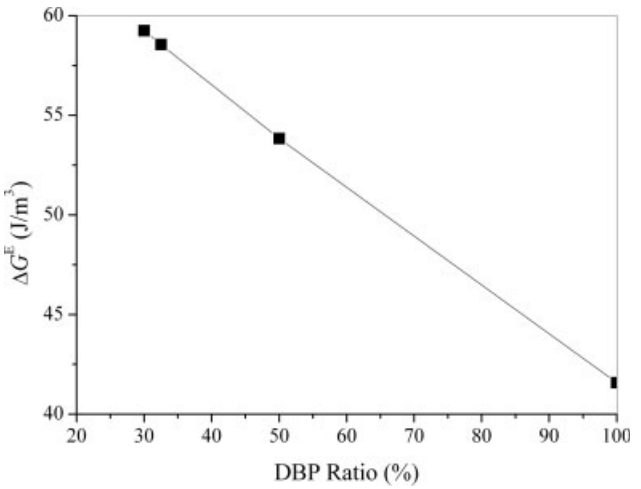

Figure 3 Relation between DBP ratio in diluent mixture and molar excess free energy of mixing (ΔG^E).

In the case of the dliuent-mixture of 40 wt/60 wt DBP/DEHP, the L-L phase separation was not observed at all under optical microscopy. The L-L phase separation maybe shift below the S-L phase, as was predicted by Burghardt,[22] and can not be observed before crystallization as shown in Figure 2. It was indicated that the crystallization temperature increased with decrease in the DBP ratio and with increase in the polymer concentration. To exhibit the phase behavior of the blend relative to the DBP ratio in diluent mixture, molar excess free energy of mixing ΔG^E involved in the blend was calculated from the Hansen solubility parameters (δ_d, δ_p, and δ_h), and then the compatibility between polymer and diluent mixture for ternary mixtures was explored.

Characterization of compatibility between polymer and diluent mixture

The estimated interaction parameter χ^* was typically used to interpret the compatibility between the polymer and the diluent, and was estimated from the difference of the Hansen solubility parameters between the polymer and the diluent using the following expression[23]:

$$\chi^* = \frac{V_m}{RT}\left[(\delta_{d1} - \delta_{d2})^2 + (\delta_{p1} - \delta_{p2})^2 + (\delta_{h1} - \delta_{h2})^2\right] \quad (1)$$

where V_m is a reference volume that equals to the molar volume of the specific repeating unit size of the polymer, δ_d and δ_p are the dispersive and the polar term of the solubility parameter, δ_h is the hydrogen-bonding contribution to the solubility parameter, and 1 and 2 refer to the diluent and polymer. By assuming that V_m is the same for every system, the compatibility between PVDF and diluent for blends at a certain temperature and the same polymer concentration can be expressed by molar excess free energy of mixing ΔG^E[24]:

$$\Delta G^E = (\delta_{d1} - \delta_{d2})^2 + (\delta_{p1} - \delta_{p2})^2 + (\delta_{h1} - \delta_{h2})^2 \quad (2)$$

Smaller values of χ^* and ΔG^E presents better compatibility between PVDF and diluent.

To validate the effects of compatibility between polymer and diluent mixture on phase diagram, four systems had been utilized (30/70, 32.5/72.5, 50/50, and 100/0 wt/wt DBP/DEHP). Subsequently, the value of solubility parameter for diluent mixture can be calculated by following:

$$\delta_i = \delta_{i1}\Phi_1 + \delta_{i2}\Phi_2 \quad (3)$$

where Φ_1 is the volume fraction of one diluent, Φ_2 is the volume fraction of another diluent and i represents d, p, and h. The values of solubility parameter for the four diluent mixtures, calculated by eq. (3) using the datum in Table I, are listed in Table II.

By solving eq. (2) with the values of solubility parameter for PVDF and diluent mixtures in Tables I and II, ΔG^E can be determined as a function of the DBP ratio in diluent mixture. Figure 3 shows that a plot of ΔG^E against the DBP ratio in diluent mixture gives a straight line. Simultaneously, it can be seen clearly that the value of ΔG^E is decreasing propor-

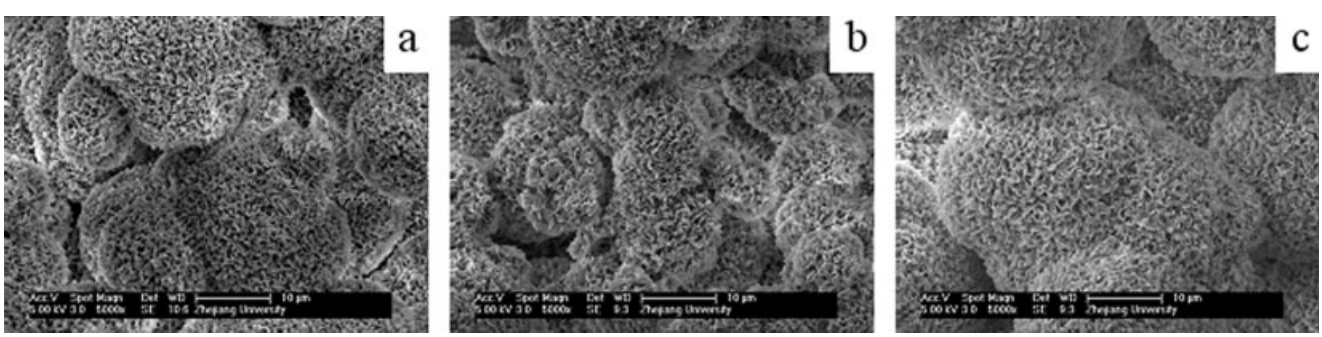

Figure 4 Micrographs of the cross sections of 30 wt % PVDF membranes. Cooling rate: 10°C/min. DBP ratio in diluent mixture: (a) 30 wt/70 wt; (b) 40 wt/60 wt; (c) 100 wt/0 wt.

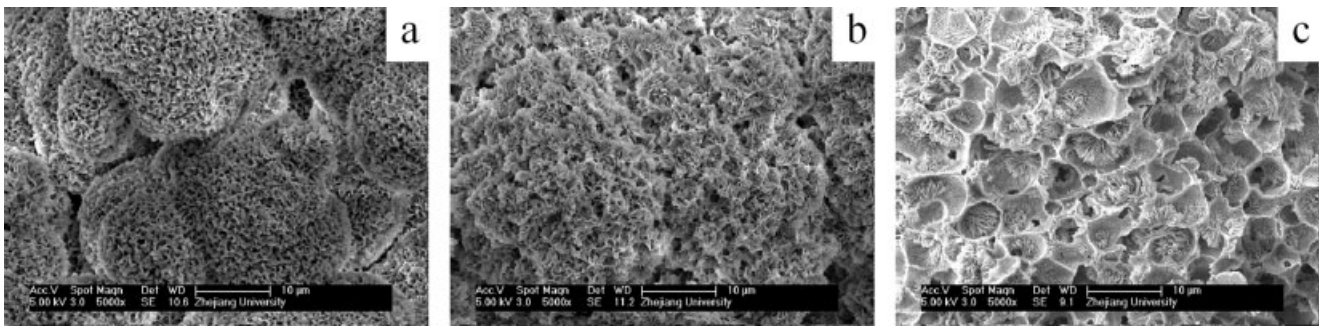

Figure 5 Micrographs of the cross sections of membranes in the system of 30 wt/70 wt DBP/DEHP. Cooling rate: 10°C/min. Polymer concentration: (a) 30 wt %; (b) 40 wt %; (c) 50 wt %.

tionally with increase in the DBP ratio in the diluent mixture, which expressed that the increase of DBP ratio in diluent mixture enhanced the compatibility between the polymer and the diluent mixture. As a result, the appearance of the L-L phase separation region above the crystallization line as shown in Figure 1 owed to the poor compatibility between polymer and diluent. For these systems with L-L phase separation, T_{cloud} decreased sensitively than T_c with the compatibility between polymer and diluent mixture increasing. As the compatibility enhanced, there was no more L-L phase separation region but only crystallization line (S-L phase separation) appearing as shown in Figure 2.

Cross-sectional structures of the PVDF membranes

The effect of the DBP ratio in diluent mixture on cross-sectional structures of membranes is shown in Figure 4. Although the L-L phase separation appeared in the cooling process for 30 wt/70 wt DBP/DEHP system, the structure of cellular pores, which is typical structure of membrane for system with L-L phase separation, was not obtained in the cross-sectional of membrane. Only closer spherulites were observed as shown in Figure 4(a). It could be explained that the cloud point was close to its T_c at 30% polymer concentration for this system as shown in Figure 1(b), and the growth of droplets during the L-L phase separation had not enough time to complete, which led to the formation of smaller droplets. The smaller droplets were arrested in spherulites during the process of PVDF crystallization. Figures 4(b,c) show the cross-sectional structures of membranes for blends at the DBP ratio of 40 wt/60 wt and 100 wt/0 wt, respectively. Relative to the system of 30 wt/70 wt DBP/DEHP, the number of spherulites increased and the size of spherulites became smaller and irregular for the system of 40 wt/60 wt DBP/DEHP, as shown in Figure 4(b). As the DBP ratio further increased, bigger and regular spherulites were formed in the system of 100 wt/0wt DBP/DEHP, as shown in Figure 4(c). While the DBP ratio increased in diluent mixture, namely the compatibility between PVDF and diluent mixture enhanced, the polymer crystallization occurred before the L-L phase separation in these two systems. Without the binary phase of rich polymer and poor polymer region taking place, the viscosity for 40 wt/60 wt DBP/DEHP system became lower relative to 30 wt/70 wt DBP/DEHP system, which enhanced the folding of polymer molecules in the crystallization and led to the formation of a plenty of primary nuclei at the beginning of crystallization. In the systems with the same polymer concentration, more primary nuclei had less polymer molecules provided for growth so that these nuclei grew up into smaller and irregular spherulites. In the case of these systems with only S-L phase sepa-

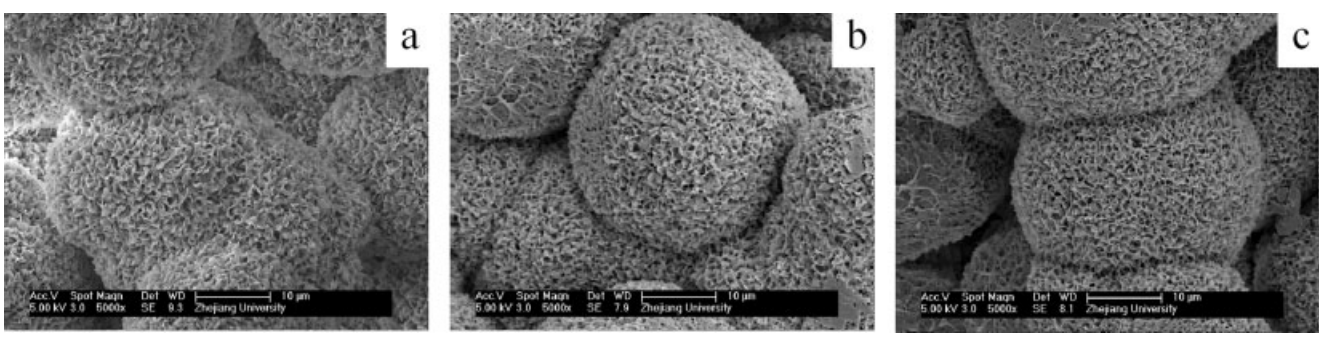

Figure 6 Micrographs of the cross sections of membranes in the system of 100 wt/0 wt DBP/DEHP. Cooling rate: 10°C/min. Polymer concentration: (a) 30 wt %; (b) 40 wt %; (c) 50 wt %.

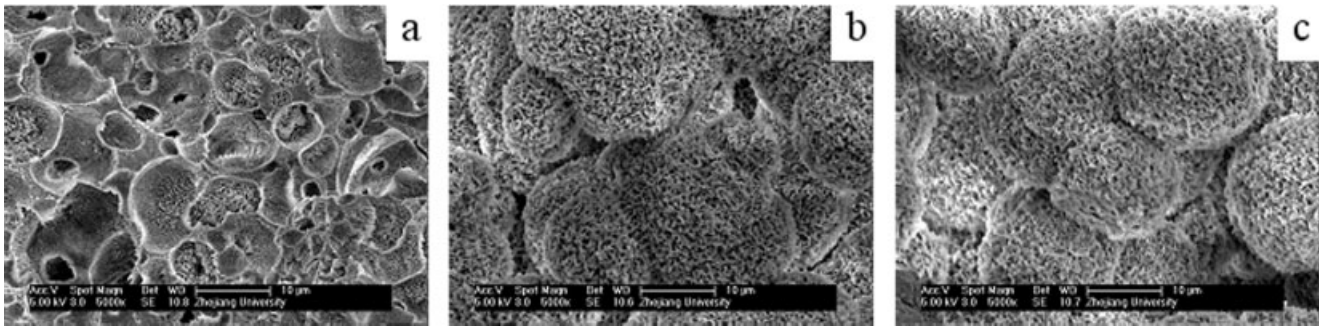

Figure 7 Micrographs of the cross sections of membranes in the system of 30 wt/70 wt DBP/DEHP. Polymer concentration: 30 wt %. Cooling rate: (a) 5°C/min; (b) 10°C/min; (c) 30°C/min.

ration, the viscosity of system and the compatibility between polymer and diluent played two critical roles in the formation of membrane morphology. DBP possesses higher viscosity than DEHP (DBP 163 mPa s (20°C) and DEHP 80 mPa s (20°C)), and so the viscosity of the system increased with the DBP ratio increasing. On the other hand, the compatibility between polymer and diluent was greatly enhanced when the DBP ratio increased from 40 wt/60 wt to 100 wt/0 wt in the diluent mixture. Both the higher viscosity of system and the stronger interaction between the polymer and the diluent prevented the nucleation activity of PVDF, which led to the formation of a few primary nuclei at the beginning of crystallization. Therefore, the cross-sectional structure of membrane for 100 wt/0 wt DBP/DEHP system presented bigger and perfect spherulites, relative to the system of 40 wt/60 wt DBP/DEHP.

The effect of polymer concentration on the cross-sectional structures of membranes is shown in Figures 5 and 6. To illustrate the evolution of the cross-sectional structures of membranes changing with the polymer concentration for the systems with L-L phase separation, a system with the diluent mixture of 30 wt/70 wt DBP/DEHP was investigated. In the case of the diluent mixture of 30 wt/70 wt DBP/DEHP, three different structures were observed with the polymer concentration increasing as shown in Figure 5. When the polymer concentration increased from 30 to 40 wt %, the structure of spherulites began to collapse, and a structure of blurry cellular pores instead of spherulites was obtained as shown in Figures 5(a,b). In Figure 5(c), cellular pores were more distinct at the polymer concentration of 50%, whereas the connectivity of the pores was unsatisfactory. The evolution of the cross-sectional structures changing with the polymer concentration for 30 wt/70 wt DBP/DEHP system was due to two factors. First, as the polymer concentration increased, there was more time for the growth of droplets due to the longer time interval while going from the cloud point to T_c as shown in Figure 1(b). Second, higher polymer concentration led to the higher viscosity which restrained the formation of spherulites. The system with 100 wt/0 wt DBP/DEHP, which underwent S-L phase separation prior to L-L phase separation, was also applied to investigate the evolution of cross-sectional structures of membranes as the polymer concentration changed. As shown in Figure 6, only structure of spherulites was obtained at various concentration of polymer, and spherulites became larger as the polymer concentration increased. Moreover, the increase of polymer concentration brought about a decrease in a space volume between spherulite.

The effect of cooling rate on the cross-sectional structures of membranes is shown in Figures 7 and 8. In the case of the diluent mixture of 30 wt/70 wt

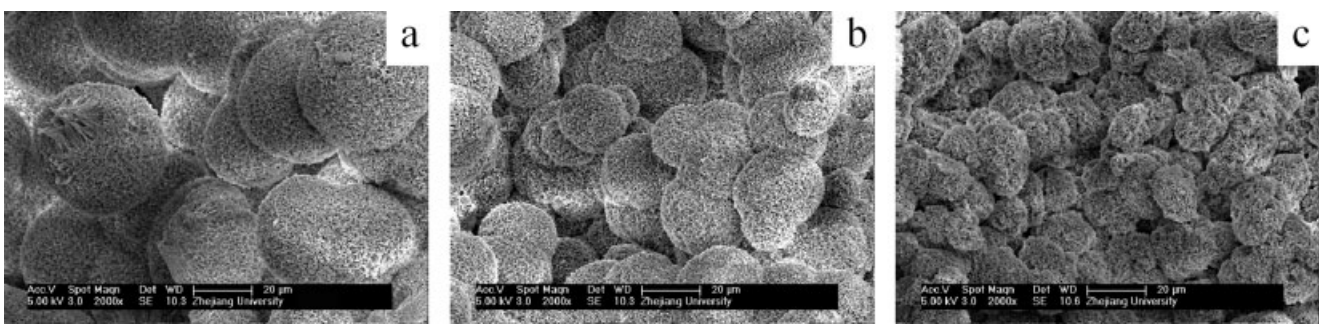

Figure 8 Micrographs of the cross sections of membranes in the system of 100 wt/0 wt DBP/DEHP. Polymer concentration: 30 wt %. Cooling rate: (a) 5°C/min; (b) 10°C/min; (c) 30°C/min.

DBP/DEHP, irregular cellular pores were observed at a cooling rate of 5°C/min as shown in Figure 7(a). When the cooling rate increased to 10°C/min, a spherulite structure appeared instead of irregular cellular pore as shown in Figure 7(b). This could be explained that droplets had enough time to grow at lower cooing rate, which resulted in the formation of big droplets. Big droplets were difficult to be arrested in spherulites and became a barrier in the formation of spherulites. As the cooling rate further increased to 30°C/min, spherulites became smaller but perfect as shown in Figure 7(c). The cross-sectional structures of membranes for the 100 wt/0 wt DBP/DEHP system at various cooling rate are shown in Figure 8. Typical structures of spherulites for S-L phase separation were obtained. The faster the cooling rate was, the smaller the spherulite size became. Both Kim[25] and Matsuyama[26] reported similar experimental results in that the crystal size was smaller in the faster cooling condition for isotactic polypropylene and poly(ethylene-*co*-vinyl alcohol) in polymer–diluent blends, respectively. Higher cooling rate seems to be advantageous for nucleation of polymer at the primary stage of crystallization, whereas the initial polymer concentration is constant. These two factors lead to the smaller spherulite at higher cooling rate.

CONCLUSIONS

Dynamic phase diagrams for PVDF in the diluent mixtures of DBP and DEHP were determined by an optical microscope and DSC. It was successful to control systematically liquid–liquid (L-L) phase separation and solid–liquid (S-L) phase separation by changing the ratio of DBP in diluent mixture. All the phase diagrams in which L-L phase boundary occurs showed that the cloud point curve shifted to lower temperatures as the DBP ratio increased, while the crystallization curve changed little. In the phase diagram for the system with only S-L phase separation, it was found that the crystallization temperatures increased with decrease in the DBP ratio and with increase in the polymer concentration. All the phase behaviors of the blends relative to DBP ratio was characterized by molar excess free energy of mixing (ΔG^E) involved in the blend. It was explored that when the DBP ratio increased, the compatibility between PVDF and diluent mixture enhanced due to the decrease in the value of ΔG^E.

The effects of the DBP ratio in diluent mixture, initial polymer concentration, and cooing rate on the cross-sectional structures of membranes were investigated. When the polymer concentration is located at 30 wt %, only spherulites were observed in membranes formed from systems with different DBP ratios. For the system of 30 wt/70 wt DBP/DEHP with L-L phase separation, cellular pores structures were detected when the initial polymer concentration was higher or the cooling rate was slower. It was explained that if droplets had long time to coarsen, big droplets were formed and prevented spherulites from growing. In the case of the system of 100 wt/0 wt DBP/DEHP with only S-L phase separation, cross-sectional structures of membranes showed only spherulites structures, and the sizes of spherulites increased with increase in the polymer concentration and with decrease in the cooling rate.

References

1. Jian, K.; Pintauro, P. N.; Ponangi, R. J Membr Sci 1996, 117, 117.
2. Jian, K.; Pintauro, P. N. J Membr Sci 1997, 135, 41.
3. Tomaszewska, M. Desalination 1996, 104, 1.
4. Khayet, M.; Matsuura, T. Ind Eng Chem Res 2001, 40, 5710.
5. Khayet, M.; Feng, C. Y.; Khulbe, K. C.; Matsuura, T. Desalination 2002, 148, 321.
6. Tarascon, J. M.; Gozdz, A. S.; Schmutz, C.; Shokoohi, F.; Warren, P. C. Solid State Ionics 1996, 86, 49.
7. Boudin, F.; Andrieu, X.; Jehoulet, C.; Olsen, I. I. J Power Sources 1999, 81/82, 804.
8. Sugihara, M.; Fujimoto, M.; Uragami, T. Am Chem Soc Div Polym Chem Prepr 1997, 20, 999.
9. Bottino, A.; Camera-Roda, G.; Capannelli, G.; Munari, S. J Membr Sci 1991, 57, 1.
10. Cheng, L.-P.; Young, T.-H.; Fang, L.; Gau, J.-J. Polymer 1999, 40, 2395.
11. Cheng, L.-P. Macromolecules 1999, 32, 6668.
12. Bottino, A.; Capannelli, G.; Comite, A. Desalination 2005, 183, 375.
13. Yeow, M. L.; Liu, Y.; Li, K. J Membr Sci 2005, 258, 16.
14. Hiatt, W. C.; Vitzthum, G. H.; Wagener, K. B.; Gerlach, K.; Josefiak, C. ACS Symp Ser 1985, 269, 229.
15. Gu, M.; Zhang, J.; Wang, X.; Tao, H.; Ge, L. Desalination 2006, 192, 160.
16. Smith, S. D.; Shipman, G. H.; Floyd, R. M.; Freemyer, H. T.; Hamrock, S. J.; Yandrasits, M. A.; Walton, G. S. WO. Pat. 035,641 (2005).
17. Mulder, M. Basic Principles of Membrane Technology; Kluwer Academic: Dordrecht, 1996.
18. Lloyd, D. R.; Kim, S. S.; Kinzer, K. E. J Membr Sci 1990, 52, 239.
19. Kim, S. S.; Lim, B. A.; Alwattari, A. A.; Wang, Y. F.; Lloyd, D. R. J Membr Sci 1991, 64, 41.
20. Vadalia, H. C.; Lee, H. K.; Myerson, A. S.; Levon, K. J Membr Sci 1994, 89, 37.
21. Shang, M.; Matsuyama, H.; Teramoto, M.; Okuno, J.; Lloyd, D. R.; Kubota, N. J Appl Polym Sci 2005, 95, 219.
22. Burghardt, W. R. Macromolecules 1989, 22, 2482.
23. Liu, B.; Du, Q.; Yang, Y. J Membr Sci 2000, 180, 81.
24. Brandrup, J.; Immergut, E. H.; Grulke, E. A. Polymer Handbook, 4th ed.; Wiley: New York, 1999.
25. Kim, S. S.; Lloyd, D. R. J Membr Sci 1991, 64, 13.
26. Matsuyama, H.; Iwatani, T.; Kitamura, Y.; Tearamoto, M.; Sugoh, N. J Appl Polym Sci 2001, 79, 2449.